Poly(α-vinyl-ω-alkyloligothiophene) Side-Chain Polymers. Synthesis, Fluorescence, and Morphology

Manuela Melucci,[†] Giovanna Barbarella,*[,†] Massimo Zambianchi,[†] Mario Benzi,[†] Fabio Biscarini,[‡] Massimiliano Cavallini,[‡] Alessandro Bongini,[§] Serena Fabbroni,[§] Marco Mazzeo,[⊥] Marco Anni,[⊥] and Giuseppe Gigli[⊥]

CNR-ISOF and CNR-ISMN-Sez BO, Via Gobetti 101, 40129 Bologna, Italy; Dip. Chimica G. Ciamician, Univ. Bologna, Via Selmi 2, 40126, Bologna, Italy; and NNL-INFM, Dip. Ingegneria dell' Innovazione, via Arnesano, 73100 Lecce, Italy

Received May 7, 2004

ABSTRACT: The synthesis of polyvinyl polymers by radical polymerization of α-vinyl-ω-alkyl-terminated thiophene and bi-, ter-, and quaterthiophenes is reported. The photoluminescence properties of the polymers in solution and in thin film are described. In thin film, self-assembly-induced white photoluminescence was observed for poly(5-vinyl-5‴-hexylquaterthiophene). For this polymer, single crystals with rectangular shape and micrometer size were obtained by drop casting from CS_2. MM3 calculations on model diads and triads indicate that, on increasing the size of the side groups, van der Waals interactions promote the stacking of the pendants on the same side of the polyvinyl chain.

Introduction

The realization of supramolecular architectures of well-defined dimensions, shapes, and functions is one of the current challenges of research in the field of organic multifunctional materials.[1] Various approaches have been exploited to control the structure and properties of molecular and polymeric materials at the micro- and nanoscales through the manipulation of the self-assembly of the most diverse constituents. The long-term goal is the chemical control of highly complex materials obtained through the self-organization of appropriately designed components and able to perform integrated functions in given environments.

Among the most performant functional materials are π-conjugated compounds which are currently being tested in a variety of devices.[2,3] In this class, the oligomers of thiophene have been demonstrated to be among the best semiconductor[4−7] and fluorescent functional materials.[8,9]Both fluorescence and charge transport properties of these oligomers are strongly dependent on their self-assembly modalities.

The oligomers of thiophene tend to form aggregates, and in the solid state they display a great diversity of conformation and packing.[10] The nature of the interactions driving the self-assembly of these compounds is not yet well understood. Since the electronegativity of sulfur is very close to that of carbon, there are not hydrogen-bonding interactions of the type as those observed, for example, in polypyrroles as a recurrent motif involving the nitrogen atom.[11] The analysis of the conformation and packing in single crystals of thiophene oligomers indicates that both are determined by the interplay of numerous, weak, and directional interactions (S···S, C−H···S, C−H···π, van der Waals and stacking interactions) whose balance varies case by case.[12] There are conflicting requirements for the optimization of charge transport or fluorescence in these compounds, as optimization of charge transport requires crystalline morphologies, high molecular ordering, and close packing of the molecules, which are instead detrimental to fluorescence.

Scheme 1. Free Radical Polymerization of 2-Vinylthiophene with the Reaction Initiated by the Radical Initiator I[18b]

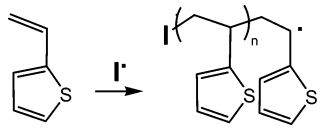

In this context, the challenge consists of devising alternative ways of manipulating the self-assembly of multifunctional thiophene oligomers in order to achieve the control of their properties. One approach is to interconnect thiophene oligomers by means of a polyvinyl chain to generate polymers with a structure similar to that of poly(*N*-vinylcarbazole), a well-known electroactive polymer whose morphology can be oriented by the choice of appropriate experimental conditions.[13] More recently, new families of polyvinyl polymers with bulky pendant groups have been described, whose supramolecular self-assembly properties are tuned via the appropriate choice of the side groups.[14−16] It is likely that, when interconnected by a polyvinyl chain, thiophene oligomers interact with modalities different from those typical of the free oligomers, owing to the steric constraints imposed by the repetition period of the structure, thus leading to the expression of new and attractive properties.

Poly(2-vinyl-5-methylthiophene) was first prepared by Trumbo[17] by free radical polymerization of the vinyl precursor and demonstrated to be an atactic polymer by proton and carbon-13 NMR. Later, Fernandez et al.[18] reported a detailed laser desorption mass spectrometry study aimed at the comparison of poly(2-vinylthiophenes) obtained by electrochemical and by classical benzoyl peroxide-initiated polymerizations. They demonstrated that the electrochemical preparation yields a polymer with a consistent amount of cross-linking while the chemical preparation takes place by the well-established free radical chain propagation mechanism, leading to the formation of the polyvinyl polymer

[†] CNR-ISOF.
[‡] CNR-ISMN-Sez BO.
[§] Univ. Bologna.
[⊥] NNL-INFM.
* Corresponding author. E-mail barbarella@isof.cnr.it.

10.1021/ma049102q CCC: $27.50
Published on Web 07/01/2004

Scheme 2. Synthesis of PT1Me, PT2Me, and PT3Me[a]

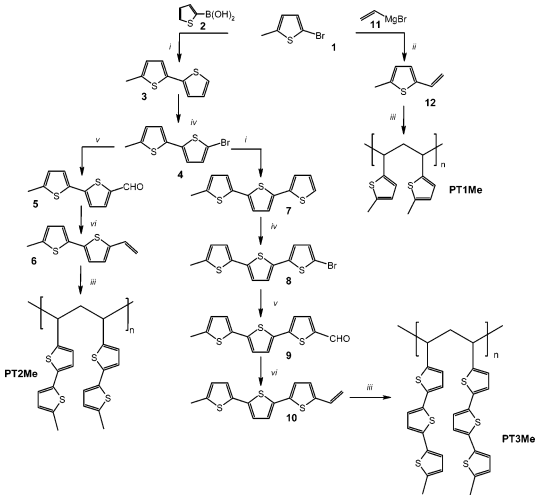

[a] (i) $PdCl_2$dppf, KF, toluene−methanol, μν; (ii) $NiCl_2$dppp, THF; (iii) BPO, neat, 90 °C, 16 h; (iv) NBS, DMF; (v) BuLi, DMF, THF; (vi) CH_3BrPPh_3, BuLi.

depicted in Scheme 1, mainly terminated by chain transfer.[18b] More recently, a few authors have described the preparation of doped polyvinyl polymers with pendant thiophene oligomers by electrochemical oxidative polymerization of vinyl precursors, aimed at obtaining new classes of electrochromic polymers.[19−22]

On these grounds, we have synthesized new α-vinyl oligomers, capped at the ω-position with alkyl groups, and carried out radical-initiated addition polymerization of these compounds. We provide experimental evidence of the polyvinyl structure of the polymers and show that this class of materials exhibits interesting fluorescence emission properties and the possibility to obtain three-dimensionally ordered structures by the proper choice of oligomer size and alkyl terminating groups.

Results

I. Synthesis and Characterization. The pattern followed for the preparation and the polymerization of vinyl-terminated mono-, bi-, ter-, and quaterthiophenes is described in Schemes 2 and 3. To prevent cross-linking during the polymerization process, all starting materials were capped with a terminal alkyl group, either methyl or *n*-hexyl.

2-Vinyl-5-methylthiophene, **12**, was prepared by action of vinylmagnesium bromide on commercial 2-bromo-5-methylthiophene, and the yield obtained after distillation (39%) was slightly higher than that obtained from other methods.[18] The synthesis of the oligomers was carried out by means of Suzuki or Stille couplings in the presence of palladium catalysts.[23] In a few cases we took advantage of microwave assistance.[24]

Polymers **PT2Me**, **PT3Me**, **PT3Hex**, and **PT4Hex** are new compounds while **PT1Me** had already been prepared both electrochemically and chemically.[18] Since 2-vinyl-5-methylthiophene and 5-vinyl-5′-methyl-2,2′-bithiophene were obtained in the form of viscous oils, polymers **PT1Me** and **PT2Me** were synthesized in the

Scheme 3. Synthesis of PT3Hex and PT4Hex[a]

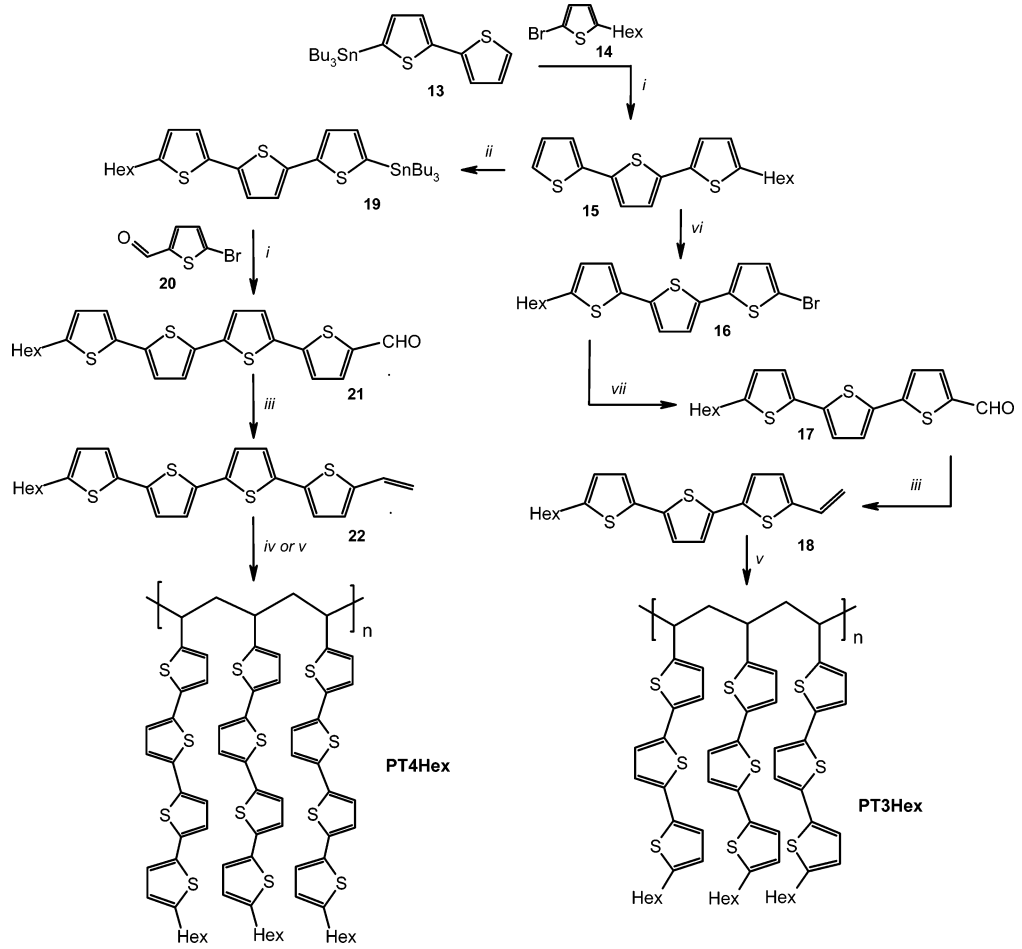

[a] (i) $Pd(AsPh_3)_4$, toluene; (ii) BuLi, Bu_3SnCl, Et_2O; (iii) CH_3BrPPh_3, BuLi; (iv) AIBN, toluene, reflux; (v) spontaneous polymerization in air; (vi) NBS, DMF; (vii) BuLi, DMF, THF.

Table 1. Proton[a] and Carbon-13[a] NMR Spectra and Molecular Weights[b] of Aliphatic Polymers

polymer	^{1}H NMR	^{13}C NMR	M_w	M_n	M_w/M_n
PT1Me	1.3−1.7 (CH_2)	15.4 (CH_3)	4700	2800	1.7
	2.2−2.7 (CH_3,CH)	36.8; 36.3 (CH)			
		45.9[d]; 29.7 (CH_2)			
	5.9−6.5 (CH)[c]	123.8; 124.0 (CH)[c]			
PT2Me	1.4−1.7 (CH_2)	15.3 (CH_3)	3800	1700	2.2
	2.3−2.6 (CH_3, CH)	36.5; 36.6; (CH)			
		45.4[c] (CH_2)			
	6.0−6.9 (CH)[c]	122.4; 122.9; 125.8 (CH)[c]			
PT3Me	1.2−1.5 (CH_2, CH)	15.4 (CH_3)	760	670	1.2
	2.4−2.6 (CH_3)	26.6; 27.2; (CH)			
	6.5−7.2 (CH)[c]	27.7; 28.1;			
		45.5; 45.9;			
		46.6			
		27.1; 29.7 (CH_2)			
		45.1; 45.2			
	126.0; 123.5 (CH)[c]				
PT3Hex	0.89 (CH_3)				
	1.26; 1.31; (CH_2, CH)	14.1 (CH_3)	5100	2800	1.8
	1.57; 1.66;				
	2.77 (CH_2)				
	6.5−7.1 (CH)[c]	22.6; 28.8 (CH_2)			
		29.7; 30.2			
		31.6			
		122.0; 125.0 (CH)[c]			
PT4HexA	0.94 (CH_3)		1500	1000	1.5
	1.27; 1.35; (CH_2, CH)				
	1.41; 1.69; 1.70				
	2.79; 2.81 (CH_2)				
	6.5−7.1 (CH)[c]				
PT4HexB[e]	0.92−0.95 (CH_3)				
	1.1−1.5; (CH_2, CH)				
	1.61; 1.68				
	2.76 (CH_2)				
	6.4−7.8 (CH)[c]				

[a] In $CDCl_3$. [b] Gel permeation chromatography using toluene as the eluant. [c] Aromatic protons. [d] Center of a broad multiplet. [e] In $CDCl_3$/CS_2.

absence of solvents, under a nitrogen atmosphere, using benzoyl peroxide (BPO) as the radical initiator, according to the modalities reported for the preparation of poly(2-vinylthiophene).[18] Instead, since 5-vinyl-5″-methyl-2,2′;5′,2″-terthiophene is a solid compound, **PT3Me** was prepared in dry and degassed toluene, under a nitrogen atmosphere, using 2,2′-azobis(isobutyronitrile) (AIBN) as the radical initiator.

Polymers **PT3Hex** and **PT4HexA** were obtained by spontaneous polymerization in air of the corresponding vinyl monomers, **18** and **22**, at room temperature and in the absence of solvents.

The spontaneous bulk polymerization of **18** and **22** was a slow process of which we became aware weeks after the preparation and purification of the monomers. The polymers obtained in this way were first quenched in methanol and then repeatedly washed with organic solvents to eliminate the residual monomer. To compare the structure of the polymers obtained by spontaneous polymerization with that of the polymers obtained using a radical initiator in solution, we prepared polymer **PT4HexB** in dry and degassed toluene, under a nitrogen atmosphere, using azobis(isobutyronitrile) (AIBN) as the radical initiator.

The polymers were characterized by gel permeation chromatography (GPC) using polystyrene as the standard and toluene as the eluant (GPC plots are reported as Supporting Information). Weight-average molecular weights and polydispersity indexes are given in Table 1. Since the repeat unit mass of **PT1Me** is 124 Da, the M_w value of this polymer corresponded to more than 40 repeat units, in good agreement with the polymer obtained by Fernandez et al.[18] **PT2Me** (repeat unit mass 152 Da) was characterized by more than 25 repeat units. For **PT3Me** (repeat unit mass 287 Da) the M_w value corresponded to 3−4 repeat units. However, **PT3Me** is much less soluble than **PT1Me** and **PT2Me**, and most likely, the molecular weight obtained from GPC is relative to the most soluble fractions. The GPC measurements of the spontaneously formed polymers gave for **PT3Hex** (repeat unit mass 358 Da) 14 repeat units and for **PT4HexA** (repeat unit mass 440 Da) only 3 repeat units. Once again, since these polymers are only scarcely soluble in toluene, the GPC reflects the characteristics of the most soluble fractions. **PT4HexB** was insoluble in toluene and could not be characterized by GPC. However, this polymer was soluble in CS_2, and it could be characterized by ^{1}H NMR using a diluted mixture of CS_2 and $CDCl_3$.

With regards to the GPC measurements, it should be noted that polystyrene becomes progressively a less suitable standard as the pendant size increases; hence, the number of repeat units for the polymers with the longer pendants has to be taken as only indicative. This is certainly a point to set in future studies, together with the standardization of polymerization methods. All polymers showed great chemical stability and were kept in air for many months without any appreciable alteration.

The structural regularity of the polymers was demonstrated by their proton and carbon-13 NMR spectra. The ^{1}H and ^{13}C NMR characteristics of the polymers are given in Table 1. The assignments were based on routine monodimensional (DEPT) and bidimensional spectra (COSY, *ghsqc*). The table shows that the proton and carbon-13 NMR chemical shifts of all polymers are

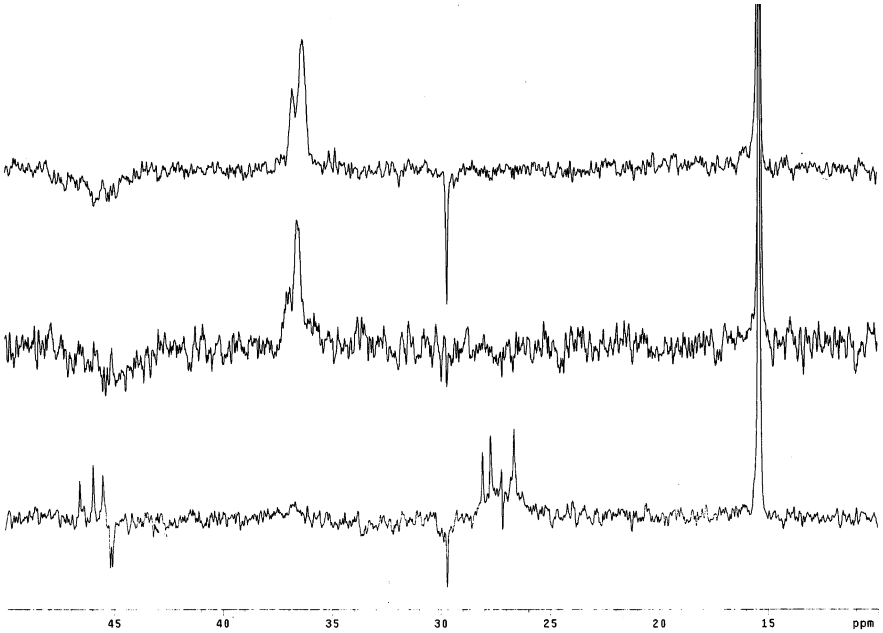

Figure 1. ^{13}C NMR DEPT spectrum of **PT1Me**, **PT2Me**, and **PT3Me** (from top down) showing the −CH (up) and $-CH_2$ (down) signals of the polyvinyl chain. The intense signal at 15.3 ppm is due to the $-CH_3$ groups which have the same chemical shifts in the three poymers.

very similar. The dispersion of proton and carbon-13 signals is in agreement with the atactic nature of these polymers.[17] The ^{13}C signals pertaining to the methylene and methyne groups of the polyvinyl chain were well resolved in the spectrum of **PT3Me**, since this polymer is made of only a few repeating units. The ^{13}C NMR region of these signals is reported in Figure 1, together with the corresponding region of polymers **PT1Me** and **PT2Me**. It is seen that, in agreement with the much greater chain length of these polymers, the −CH and $-CH_2$ signals do not display sharp features but a wider distribution of chemical shifts following within the same spectral region, due to slightly different chemical environments. Very significantly, **PT4HexA** and **PT4HexB** displayed very similar proton spectra, dominated by the intense signals of the hexyl chains and characterized by the same spectral regions as the polymers with the pendants terminated by a methyl group. For **PT3Hex** it was also possible to obtain the ^{13}C NMR spectrum, whose signals followed in the same region as that of the methylated polymers.

The structural regularity of the polymers described above is confirmed by the optical properties reported in section II.

II. Optical Properties. The normalized absorption spectra of **PT1Me**, **PT2Me**, **PT3Me**, **PT3Hex**, and **PT4HexA** in chloroform (∼0.1 mg/mL) are reported in Figure 2. All spectra are characterized by broad and featureless bands with line shape and maximum absorption wavelength reflecting the optical features of the side-chain groups. In particular, a progressive red shift from 250 to 425 nm is observed on increasing the pendant size from thiophene to quaterthiophene, in agreement with the absorption wavelength shifts of the corresponding oligomers in solution.[25] For all polymers the main band is always accompanied by a broad, bathochromically shifted, and very low-intensity band.

Upon UV−vis irradiation, all polymers, including **PT1Me**, show fluorescence emission in the visible region, with a progressively red-shifted wavelength as the pendant size increases, in agreement with the trend

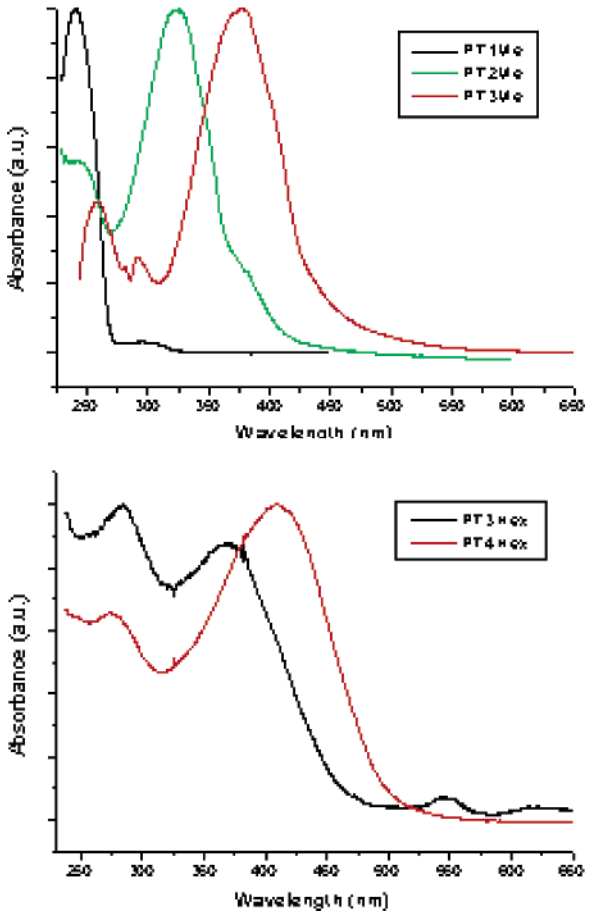

Figure 2. Absorption spectra of polymers **PT1Me**, **PT2Me**, **PT3Me** (top) and **PT3Hex**, **PT4HexA** (bottom) in $CHCl_3$ (∼0.1 mg/mL).

shown by thiophene oligomers in solution.[25] The PL spectra of all polymers in solution are markedly dependent on concentration and are generated by a complex pattern of intra- and interchain interactions between pendants. The trend is illustrated for **PT1Me**

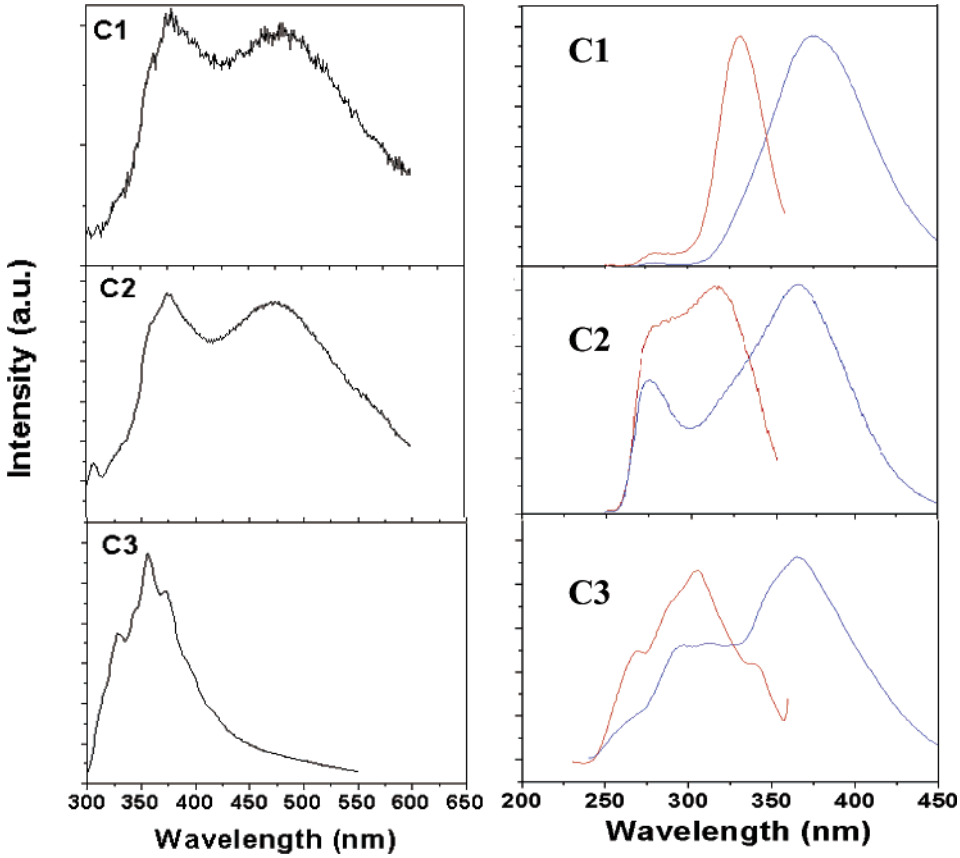

Figure 3. Left: photoluminescence spectra of **PT1Me** on changing the concentration in $CHCl_3$, from C1 = 1 mg/mL to C2 = 0.1 mg/mL and C3 = 0.01 mg/mL. Right: PLE spectra at 350 nm (red) and 475 nm (blue).

in Figure 3, showing the photoluminescence (PL) and photoluminescence excitation (PLE) spectra on varying the concentration of the polymer in chloroform from C1 (1 mg/mL) to C2 (0.1 mg/mL) and C3 (0.01 mg/mL).

At high concentrations, C1 and C2, the PL spectrum consists of two intense, broad and unstructured bands, peaked at 375 nm (S1, 3.31 eV) and 475 nm (S2, 2.61 eV). On diluting the solution, S2 almost vanishes, whereas S1 remains intense although modified in shape.

The band S1 is present at all concentrations, indicating that it is mainly due to the interactions between pendants belonging to the same chain. The PLE spectra show that S1 originates from an electronic state at 3.81 eV, with contributions from a higher energy state at 4.5 eV when the solution is diluted. The variations observed in the PLE spectra for the emission peak at 375 nm (S1) show also that the monomers interact in different ways on varying the concentration.

The S2:S1 relative intensity shows a strong increase with the concentration, indicating that S2 band arises mainly from aggregation states with an interchain origin. The PLE spectra at different concentrations show that these aggregates can be directly excited at 3.3 eV (375 nm) and also through higher energy states at 4.5 eV (275 nm) and 3.81 eV (325 nm), coinciding with the excitation energy of the S1 emission.

The relaxation dynamics of the S2 band has been studied by time-resolved spectroscopy by exciting the solutions at 3.18 eV (390 nm, direct aggregate excitation) at concentration C1. The relaxation dynamics is biexponential with a fast decay time of 210 ± 10 ps and a slow decay time of 2200 ± 200 ps. Such a nonexponential decay with a long decay time is typical of disordered aggregate states.

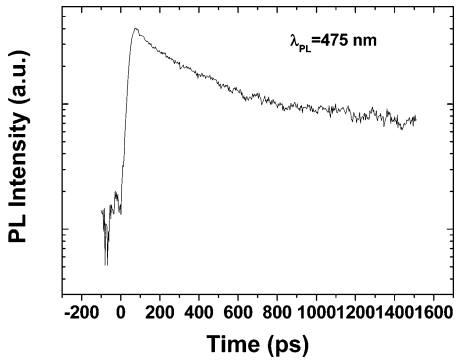

Figure 4. Fluorescence relaxation dynamics of **PT1Me** at 475 nm and concentration C1.

Similar, albeit more complex, photoexcitation dynamics was observed for the other polymers and will be described in detail in forthcoming papers.

Figure 5 shows the PL spectrum of polymer **PT4HexA** in high concentration (≈1 mg/mL) solutions and in spin-coated film on a glass substrate. The PL spectrum in solution is quite broad (it covers almost the entire visible range) with structures at 467, 500, and 540 nm, reminiscent of the vibronic bands present in the spectrum of α-quaterthiophene in solution.[25a−c] We attribute these features to the superposition of the signals originating from isolated quaterthiophene molecules (i.e., weakly interacting pendants) and lower energy emitting aggregates. PLE spectra (not reported) show that the emission band at 467 nm mainly originates from an electronic state at 3.31 eV (375 nm) with weaker contributions from an electronic state at 4.51 eV (275 nm), whereas the emissions at 500 and 540 nm originates from an electronic state near 460 nm.

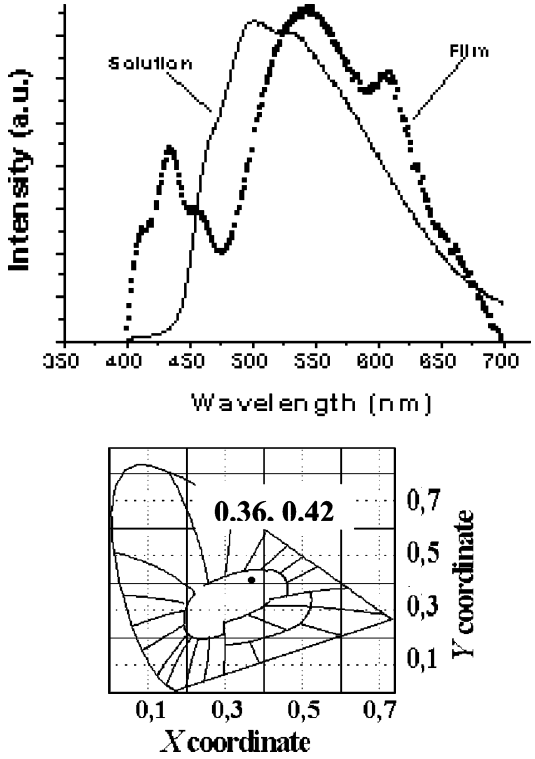

Figure 5. Top: PL spectrum of **PT4HexA** at high concentration (≈1 mg/mL) in chloroform and in spin-coated film. Bottom: CIE photometric coordinates of the spin-coated film, corresponding to white light emission.

The spectrum of **PT4HexA** in the solid state is more structured than that in solution and presents two additional sharp bands at 430 and 630 nm. The presence of these two extra bands in the blue and red regions results in an overall white light emission, as shown by the CIE[28] coordinates (0.36, 0.42) of the chromaticity diagram reported in Figure 5. The PLE spectrum of the film (not reported) shows that the highest energy bands of the PL spectrum (at 430 nm) originate from two electronic states at 4.51 eV (275 nm) and at 3.31 eV (375 nm).

III. Polarized Optical Microscopy and Atomic Force Microscopy (AFM). Optical microscopy imaging of spin-coated films of all polymers, deposited on glass from $CHCl_3$/ CS_2 or CS_2 solutions, showed the films to be amorphous, as they did not display any birefringence when examined with crossed polarizers. However, the films deposited on glass by drop casting of **PT4HexA** and **PT4HexB** (estimated concentration ≈ 10^{-5}−10^{-6} M) besides the amorphous phase showed also the presence of some birefringent crystalline aggregates, which were then imaged by atomic force microscopy (AFM). The sizes of the crystals obtained by drop casting of **PT4HexA** and **PT4HexB** were variable in a range between a few μm and more than 100 μm with a mean length of 40 μm. We did not observe any special orientation of the crystals with respect to the substrate. The crystals' shape appeared to be rectangular with an angle of 90 ± 0.5°. The crystals' color ranged from violet to yellow depending on their thickness. The crystals showed the same color both under ordinary illumination and under polarized light.

The investigation by microscope with crossed polars showed optical anisotropy of the crystals, which appeared colored under crossed polars, whereas the amorphous film was dark. By rotating the microscope stage

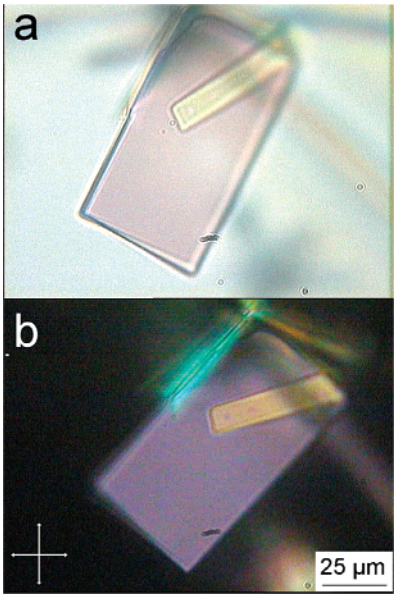

Figure 6. Optical micrographs of a **PT4HexB** crystal on glass obtained by drop casting from CS2. (a) Micrograph taken under ordinary (unpolarized) light. (b) Micrograph taken between crossed polars oriented along the axis of the image (arrows indicate the orientations of polarizer/analyzer). The crystal extinguished when crossed polars were oriented parallel or perpendicular to crystal edges and were brightest at 45 ± 1°.

(i.e., the crystal orientation with respect to the polarized light), the crystals extinguished (become dark) in four positions at intervals of 90°. (A movie of crystal behavior on changing their orientation vs the polarized light is provided as Supporting Information.) The evidence of complete light extinguishment for the same orientation in all crystals indicates that all domains have the same orientation, a behavior suggesting that every small microcrystal could be a single crystal.

Figure 6 shows one of the crystals formed by drop casting of **PT4HexB** under nonpolarized (top) and polarized (bottom) light. The crystal has a rectangular shape, and another crystal grown on it, with the same rectangular shape but rotated by 60 ± 0.5°, can be observed. Figure 7a shows the optical image of one of the largest crystals (100 μm length) formed by drop casting of **PT4HexA** under nonpolarized light. The amorphous phase around the crystal appears highly corrugated and inhomogeneous. Figure 7b−d shows AFM images taken in intermittent contact mode revealing the typical morphology of single crystals examined by AFM. On top of the crystal there are some terraces well visible in the zoom of Figure 7c. The terraces appear flat with a typical rms roughness < 1.5 Å inside the terraces, the minimum step between adjacent terraces being 1.70 ± 0.05 nm. The step corresponds to the length of the pendant.

IV. MM3 Molecular Mechanics Calculations of Model Diads and Triads SI. To analyze the conformational properties and energies of the polymers with pendant thiophene oligomers (Th), we carried out MM3[26] molecular mechanics calculations on the model diads and triads depicted in Scheme 4.

We first calculated the MM3 conformational energies (E) of all possible diads using a single thiophene ring as the pendant Th group.

Taking into account the rotations around the C2−C3 and C3−C4 bonds and the three possible energy minima, namely **a** (180°), **g** (60°), and **-g**(−60°), there are six

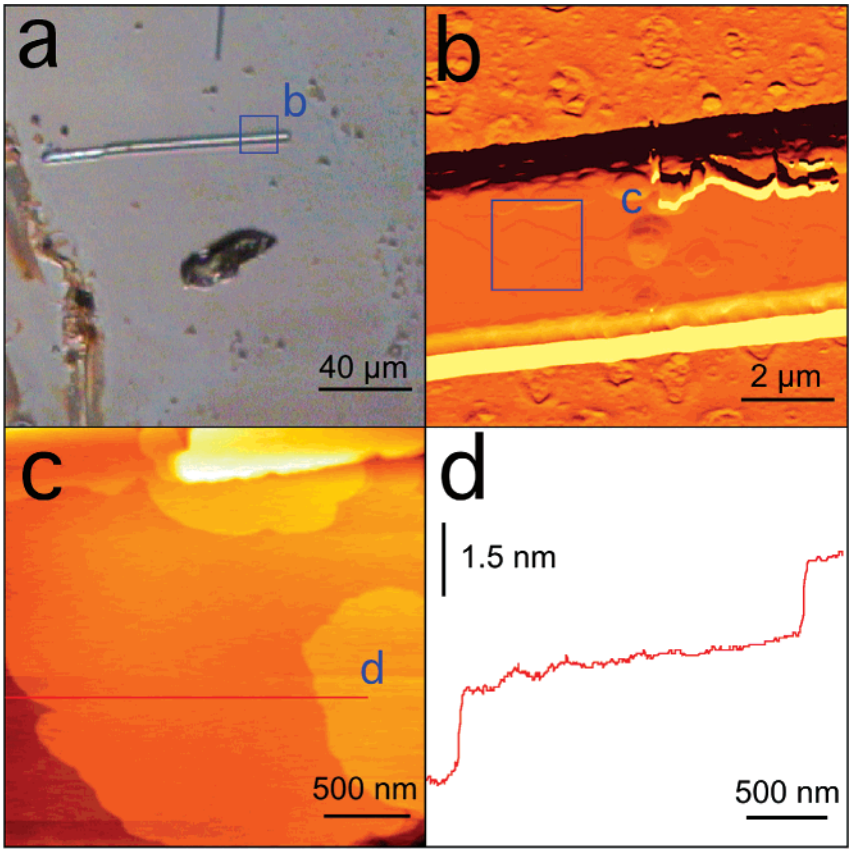

Figure 7. (a) Optical micrograph of a **PT4HexA** crystal under ordinary light. (b) AFM error signal image measured on the marked zone in part a. (c) AFM topography measured on the marked zone in part b. (d) Profile along the solid line shown in part c; the smallest terrace step is 1.70 ± 0.05 nm, which is consistent with the length of an individual pendant.

Scheme 4. Diads and Triads Taken as Models of Polymers with Pendant Thiophene Oligomers (Th)[a]

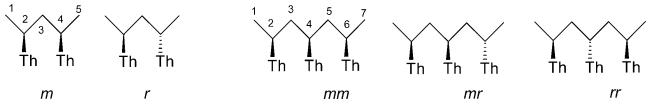

[a] m stands for *meso* and r for *racemic*.

nonequivalent conformations for both the *meso* (**aa**, **ag** ≡ **-ga**, **a-g** ≡ **ga**, **gg** ≡ **-g-g**, **g-g**,**-gg**) and *racemic* (**aa**, **ag** ≡ **ga**, **a-g** ≡ **-ga**, **gg**, **g-g** ≡ **-gg**, **-g-g**) diads. Moreover, the sulfur atom of the thiophene ring, which for steric reasons is nearly perpendicular to the polyvinyl chain, can be either on the same side (let us call this orientation: d) or on the opposite side (let us call this orientation: p) of the corresponding C−H bond. Consequently, for each possible conformation, **ag** for example, four possibilities, namely **ag**pp, **ag**pd, **ag**dp, and **ag**dd, have to be taken into account.

According to MM3 calculations, for both *m* and *r* configurations, the most stable conformations are the **aa** ones, followed by the **ag** ones, all the other conformations being higher in energy by up to 10 kcal/mol. The energies of the most stable conformations are reported in Table 2. Boltzmann population analysis showed that the preference for the **aa** conformations was 75% of the population of *m* diads and 97% of *r* diads.

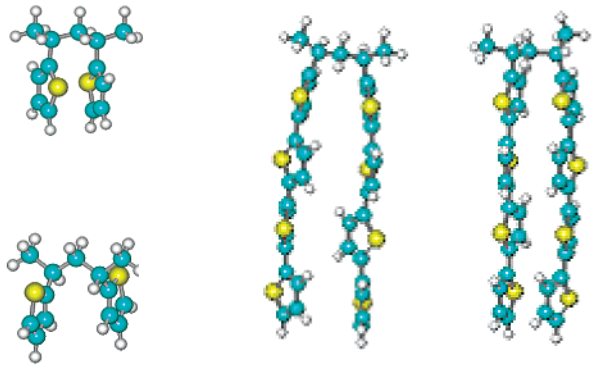

Figure 8. MM3 calculated geometry of the most stable diads with pendant thienyl and quaterthienyl groups.

These results indicate that, when the pendant Th is a single thienyl ring, the conformational preferences of the diads are dictated by the preference of the polyvinyl chain for the extended zigzag conformation. Figure 8 (left) shows the geometry of the most stable *meso* and *racemic* diads.

We then calculated the energies of the diads with pendant quaterthienyl moieties. For simplicity, only

Table 2. MM3 Calculated Conformational Energies for the *Meso* (E_m, kcal mol^{-1}) and *Racemic* (E_r, kcal mol^{-1}) Diads with a Pendant Thiophene Ring

conformation	E_m	E_{vdW}	E_r	E_{vdW}	conformation	E_m	E_{vdW}	E_r	E_{vdW}
aapp	42.8	−2.8	41.1	−1.9	**ag**pd	43.2	−1.6	44.8	−2.4
aapd (**aa**dp)	41.9	−3.1	41.4	−2.2	**ag**dp	43.0	−1.5	42.8	−2.7
aadd	43.2	−3.5	42.5	−2.4	**ag**dd	42.9	−1.5	45.7	−2.7
					agpp	42.6	−1.2	43.7	−2.5

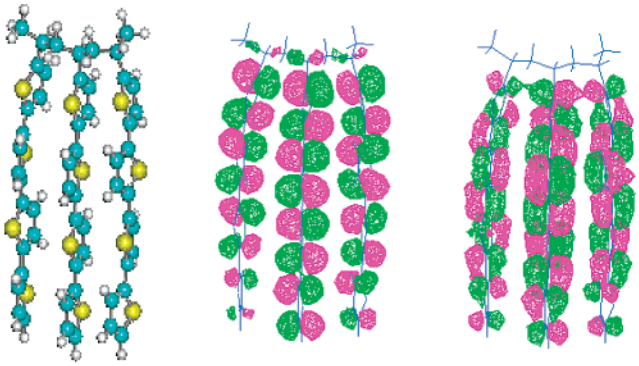

Figure 9. Geometry of the mr **aaag**ppd MM3 calculated triad with pendant all-trans quaterthienyls groups and ZINDO/S calculated shape of the frontier orbitals.

Table 3. Total Energy (E, kcal mol^{-1}) and van der Waals Contributions (E_{vdW}, kcal mol^{-1}) for the Most Stable Triads with Pendant All-Anti Quaterthienyls

conformation	E	E_{vdW}	conformation	E	E_{vdW}
mm **aaaa**ppp	256.4	−32.7	*rr* **aga-g**ppp	262.5	−28.7
mr **aaag**ppd	256.1	−32.6	*rr* **aaag**ppp	280.7	−4.7

quaterthienyls with the rings in the all-anti orientation were taken into account. Figure 8 (right) shows the geometry of the most stable quaterthienyl diads. We found that that in the *meso* form **aa** type conformations are favored, namely **aa**pd (E_m = 173.4 kcal mol^{-1}), **aa**dd (E_m = 174.8 kcal mol^{-1}), and **aa**pp (E_m = 174.2 kcal mol^{-1}), all the other conformations being higher in energy up to 15 kcal mol^{-1}. Instead, in the *racemic* form, **ag** type conformations are favored, namely **ag**pd (E_m = 175.1 kcal mol^{-1}) and **ag**pp (E_m = 177.4 kcal mol^{-1}), the **aa** forms being at least 10 kcal mol^{-1} higher in energy. Analysis of the energy components showed that the **aa** conformation in the *meso* form and the **ag** conformation in the racemic form are stabilized by van der Waals interactions amounting to about 15 kcal mol^{-1}. These interactions are due to the fact that in *m* **aa** and in *r* **ag** conformations the aromatic moieties are stacked. When the pendant group is a single thienyl ring, the energy of van der Waals interactions amounts to only −2 kcal mol^{-1} and is not sufficient to counteract the preference of *r* diads for **aa** conformations. However, when the pendant group is a quaterthienyl, van der Waals interactions become the driving force for the conformational preferences.

As far as the triads are concerned, there are 648 possible conformations for each one of them. Even taking into account that some of them are equivalent, they are too numerous for all of them to undergo calculation. Thus, we limited the calculations to a selected triad with pendant, stacked, quaterthienyls for each configuration, namely the **aaaa** conformations of the *mm* triads, the **aaag** conformations of the *mr* triads, and the **aga-g** conformations of the *rr* triads. The results are shown in Table 3, in which the energy of a conformation with minimum stacking (*rr* **aaag**ppp) is also reported for comparison, while the geometry of the most stable triad is shown in Figure 9 (left).

To have an idea of the shape and energy of frontier orbitals in triad *mr* **aaag**ppd, we carried out ZINDO/S calculations using the MM3 geometry. Figure 9 shows the frontier orbitals of the triad. Although the three pendants are separated by the aliphatic linker, their proximity and their relative orientation causes the π orbitals to overlap. Consequently, the charge appears to be delocalized on all the thiophene rings of the triad. Such a delocalization is confirmed by the calculated values of the energy of the frontier orbitals. The calculated HOMO and LUMO energies of the triad were indeed −6.13 and −0.91 eV, respectively. The ZINDO/S energies calculated for isolated quaterthiophene in the all-anti MM3 geometry were −6.46 and −0.72 eV, respectively. Thus, the triad displays the electronic properties of a system more delocalized than isolated quaterthiophene, in particular a smaller ionization potential and a greater electron affinity. Electrochemical studies of polymer **PT4Hex** are currently under way.

Discussion

Our data show that, contrary to thiophene oligomers, in which the absorption and fluorescence processes involve the same electronic states,[25] the photoexcitation dynamics of the new class of polymers is much more complex due to the interactions among different pendants. The PL and PLE spectra on increasing the pendants size and varying the concentration indicate, in fact, that there are at least three different types of contributions: (1) from energy levels generated by interchain interactions between pendants; (2) from energy levels generated by intrachain interactions between pendants; (3) from energy levels pertaining to individual pendants. The first type of contribution determines red-shifted fluorescence bands, as is generally observed in oligothiophene aggregates.[25] These PL signals are strongly dependent on concentration, since interchain aggregates disrupt as the concentration decreases (Figure 3). The second type of contribution is also related to the concentration of the polymer, since intrachain aggregates are affected by the morphology of the polymer, which is concentration-dependent. The PL emission originated by this type of aggregate is present at all concentrations with features related to the characteristics of the aggregates (Figure 3). The third type of contribution is due to noninteracting or slightly interacting pendants; thus, it is an intrinsic property not depending on concentration. A detailed analysis of the different contributions is beyond the scope of the present paper and will be the matter of future works.

The PL and PLE spectra allow a three energy levels scheme to be drawn for the photoexcitation dynamics of these polymers. Figure 10 shows the scheme for compound **PT1Me**. S2 (475 nm) is the energy level pertaining to interchain aggregates, which is absent in dilute solution and whose decay is concentration dependent and nonexponential (Figures 3). This level has three different population mechanisms: by direct excitation (380 nm), by excitation transfer from the emitting state S1 (375 nm), and from the nonemitting state S3 (275 nm). In turn, S1 is an energy level generated by intrachain interactions among pendants and can be populated by direct excitation or by nonradiative deexcitation of S3 (corresponding to the monomer).

On increasing the pendants' size, the deexcitation processes become more complicated but always with a similar dynamics dependent on concentration. Moreover, contributions from individual pendants (noninteracting or weakly interacting ones) have to be taken into

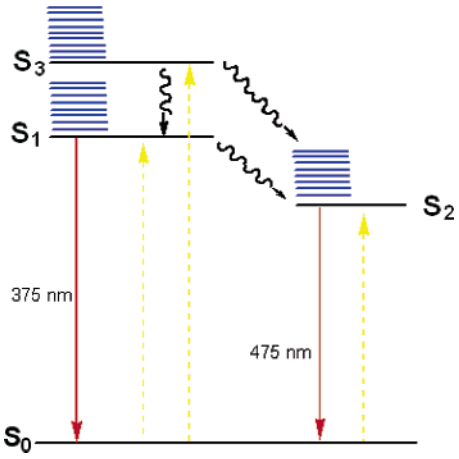

Figure 10. Scheme of the dynamics of photoexcitation of polymer **PT1Me** in solution. Absorption is indicated by yellow upward arrows and emission by red downward arrows.

account since bi-, ter-, and quaterthiophene are all light-emitting molecules.[25a]

The contribution of the individual pendants is evident in the PL emission of **PT4HexA** in solution (Figure 5), where the vibronic bands typical of α-quaterthiophene in solution characterize the spectrum at high energy and a broad emission from the aggregates characterizes the spectrum at low energy. However, the most interesting result concerning this polymer is the white light emission in the solid state. Compared to the spectrum of a thin film of dihexylquaterthiophene,[27] the spectrum of **PT4HexA** in the solid state shows additional intense and sharp bands in the blue region around 450 nm and in the red region around 620 nm. The overlap of these red and blue bands with the remaining spectrum determines white light emission, as shown by the CIE[28] coordinates of the chromaticity diagram (Figure 5). So far, only very few cases of white light emission from single polymers have been reported.[29] These kinds of materials are important in view of their application in white electroluminescent diodes with a single active film.[29]

The thin films of thiophene oligomers tend to be crystalline, even those obtained by spin-coating, although less ordered than those obtained by vacuum evaporation.[4−6,30] Crystalline order is very important to get high field effect charge mobilities.[4−6] However, crystalline aggregates cause PL quenching, and in fact, conventional thiophene oligomers are characterized by poor PL efficiencies in the solid state.[25] To get high solid-state PL efficiencies and good performance in electroluminescent devices, branched structures giving rise to amorphous films are required.[8]

Contrary to free oligomers, the spin-coated films of the oligomers embedded into the polyvinyl structure are amorphous and do not show any birefringence under polarized light. However, drop casting of polymer **PT4Hex** from CS_2 (a solvent which evaporates extremely rapidly) generates on the glass surface crystals of micrometer dimension and presents an unusual rectangular habit (Figures 6). AFM images (Figure 7) show the crystals displaying the terraced structure typical of single crystals, with the height of the terraces corresponding to the length of the pendants. Likewise, the crystals are due to the formation of isotactic micro-sized polymer segments,[31] with the pendants located on the same side of the plane of the alkyl chain. As indicated by MM3 calculations, according to which van der Waals interactions become the driving force determining the conformational preferences of diads and triads with pendant quaterthienyls, such exceptionally ordered structures are formed by virtue of synergical intramolecular van der Waals interactions among pendants. A contribution to the formation of the crystalline structures comes probably also from the lipophilic interactions between hexyl chains, in agreement with the fact that thiophene oligomers substituted with long alkyl chains at the terminal positions tend to form very ordered structures in the solid state.[32] Anyway, such polymeric single crystals, with stacked pendants as their shape and MM3 calculations suggest, are very suitable structures for charge transport, whose optimization requires close molecules and orbitals overlap.[4] According to ZINDO/S calculations on the triad of Figure 9, the close proximity of the pendants and their parallel orientation leads to the overlap of the π orbitals of adjacent pendants, thus allowing the delocalization of the π-electrons over the entire triad and the displacement of both frontier orbitals toward higher energies.

Conclusions

We have demonstrated that in poly(α-vinyl-ω-alkyloligothiophenes) the tendency of the side groups to self-assemble via intra- and interchain interactions generates new fluorescence properties tunable by means of changes in pendant size and substituents. In this way, from interconnected quaterthiophenes, we were able to obtain a polymer characterized by white light emission in thin film. Moreover, despite the fact that radical addition polymerization leads to atactic polymers, in appropriate conditions van der Waals forces among pendants lead to the formation of single-crystal microdomains. These microcrystals with stacked pendants have the kind of supramolecular ordering most suitable for charge transport.

There is a great variety of thiophene oligomers that can easily be incorporated into vinyl or other types of aliphatic chains. Thus, the initial results presented here open the door to the creation of a great number of new functional supramolecular structures by manipulation of the self-assembly properties of oligothiophene components.

Experimental Section

General Details. 2-Bromo-5-methylthiophene (**1**), 2-thiopheneboronic acid (**2**), vinylmagnesium bromide (**11**), and 5-bromo-2-thiophene carboxaldehyde (**20**) are commercially available compounds. Flash chromatographies were carried out using silica gel (200−300 mesh ASTM). Analytical thin layer chromatographies (TLC) were carried out using 0.2 mm sheets of silica gel 60 F_{254} and the visualization accomplished by UV light (356 and 254 nm). Microwave-assisted reactions were carried out in air using a commercial system Synthewave 402, with variable power and fixed temperature. The characterization of compounds **3**,[33] **4**,[34] **5**,[33,35] **6**,[18] **7**,[34] **8**,[34] **9**,[33] **10**,[19a] **12**,[17] **13**,[36] **14**,[36] and **15**[36] has already been reported. New preparation methods and additional characterization data for compounds **3**, **5**, and **7** as well as the synthesis of compounds **16** and **19** are given as Supporting Information.

Materials. *5-Hexyl-2,2′;5′,2″-terthiophene-5″-carbaldehyde*, **17**. To a solution of 0.42 g (1.03 mmol) of **16** in 7 mL of freshly distilled THF, 0.5 mL (1.33 mmol) of *n*-BuLi (2.5 M) was added dropwise at −78 °C. The mixture was allowed to warm to room temperature and then stirred for an additional 3 h. The red solution was cooled again to −78 °C, and 0.35 mL of dry DMF was added dropwise. After usual workup, the crude product

was chromatographed on silica gel using a mixture of petroleum ether:ethyl acetate (80:20), and 0.15 mg (40% yield) of a yellow powder (mp 116 °C) were obtained. *m/e* 359 [$M^{\bullet+}$], λ_{max} ($CHCl_3$) = 411 nm. ^{1}H NMR ($CDCl_3$): δ ppm 0.89 (m, 3H), 1.31 (m, 7H), 1.43 (m, 2H), 2.8 (t, J = 7.7 Hz, 1H), 6.71 (d, J = 4.0 Hz, 1H), 7.04 (dd, = 0.8 Hz, J = 4.0 Hz, 2H), 7.21 (d, J = 3.6 Hz, 1H), 7.25 (d, J = 3.6 Hz, 1H), 7.66 (d, J = 4.0 Hz, 1H), 9.85 (s, 1H). ^{13}C NMR ($CDCl_3$): δ ppm 182.40, 147.07, 146.72, 141.32, 133.73, 133.71, 128.78, 126.78, 126.89, 125.04, 124.023, 123.82, 123.79, 31.52, 30.19, 29.7, 28.7, 22.5, 14.06. Anal. Calcd for $C_{19}H_{20}OS_3$: C, 63.29; H, 5.59. Found C, 63.11; H, 5.60.

5-Hexyl-5″-vinyl-2,2′;5′,2″-terthiophene, **18**. To a THF solution (5 mL) of methyltriphenylphosphonium bromide (0.496 g, 1.39 mmol), *n*-BuLi (2.5 M, 0.56 mL, 1.39 mmol) was added dropwise at −20 °C under a N_2 atmosphere. After 2 h the white suspension turned to yellow, and 0.11 g (0.28 mmol) of **17** dissolved in 5 mL of THF was added. The mixture was stirred overnight and then quenched with 10 mL of NH_4Cl. After extractions with CH_2Cl_2 the combined organic phases were dried over magnesium sulfate and evaporated. Flash chromatography on silica gel using petroleum ether/ethyl acetate (90:10) afforded 66 mg (66%) as a yellow powder; mp 103 °C. *m/e* 358 [$M^{\bullet+}$]. ^{1}H NMR ($CDCl_3$): δ ppm 0.9−1.8 (m, 11H), 2.8 (t, 2H), 5.12 (d, J = 10 Hz, 1H), 5.52 (d, J = 17 Hz, 1H), 6.65−6.85 (m, 3H), 6.94−7.6 (m, 4H). ^{13}C NMR ($CDCl_3$): δ ppm 145.7, 141.9, 136.1, 137.0, 135.5, 134.4, 129.8, 126.9, 124.9, 124.3, 123.6, 123.4, 113.3, 31.6, 30.2, 29.7, 28.8, 22.6, 14.1. Anal. Calcd for $C_{20}H_{22}S_3$: C, 66.99; H, 6.18. Found: C, 67.12; H, 6.16.

5-Hexyl-2,2′;5′,2″;5″,2‴-quaterthiophene-5‴-carbaldehyde, **21**. $Pd_2(dba)_3$ (6.9 mg, 0.0067 mmol) and $AsPh_3$ (16.3 mg, 0.053 mmol) were dissolved in dry toluene (10 mL) under a nitrogen atmosphere. The solution was warmed until it became black, and then 0.17 g (0.89 mmol) of compound **20** was added. The stirred solution was allowed to reach reflux temperature, and then 0.71 g (1.15 mmol) of **19** was added dropwise. After 4 h of stirring at reflux, the reaction was quenched with water, extracted with CH_2Cl_2, and dried over Na_2SO_4. Flash cromatography on silica gel using pentane → Et_2O/pentane 3:1 → Et_2O/ CH_2Cl_2 1:1 afforded 0.34 mg (67% yield) of **21** as a yellow solid; mp 174 °C. *m/e* 442 [$M^{\bullet+}$]; λ_{max} ($CHCl_3$) = 434 nm. ^{1}H NMR ($CDCl_3$): δ ppm 0.91 (t, J = 7.22 Hz, 3H), 1.2−1.4 (m, 6H), 1.6−1.75 (m, 2H), 2.79 (t, J = 7.5 Hz, 2H), 6.69 (d, J = 3.5 Hz, 1H),7.00 (dd, J = 1.8/3.5 Hz), 2H), 7.10 (dd, J = 1.8/3.8 Hz, 2H), 7.22 (d, J = 4 Hz, 1H), 7.27 (d, J = 4 Hz, 1H), 7.66 (d, J = 3.8 Hz, 1H), 9.91 (s, 1H).^{13}C NMR ($CDCl_3$): δ ppm 14.3, 22.8, 27.0, 29.0, 30.4, 31.8, 123.65, 123.74, 124.0, 124.3, 124.9, 125.1, 127.0, 137.4, 134.3, 134.52, 134.53, 138.2, 139.3, 141.8, 146.4, 147.1, 182.7. Anal. Calcd for $C_{23}H_{22}OS_4$: C, 62.40; H, 5.01. Found: C, 62.51; H, 5.00.

5-Hexyl-5‴-vinyl-2,2′;5′,2″;5″,2‴-quaterthiophene, **22**. This compound was prepared by Wittig reaction in the same conditions described for the synthesis of compounds **18**, starting fom 0.4 (0.9 mmol) of **21**. The reaction was carried out over 24 h and then was quenched with water and extracted with CH_2Cl_2. The combined organic phase was dried over Na_2SO_4. A flash cromatography on silica gel using pentane → Et_2O/pentane 7:3 → Et_2O → Et_2O/ CH_2Cl_2 1:1 → CH_2Cl_2 gave 0.238 g (60% yield) of an intense red powder; mp 168−172 °C; λ_{max} = 413.37 nm. IR: 2940, 2926, 2856, 1650, 1480, 1443, 1380, 1264, 1097, 907, 845 cm^{-1}. ^{1}H NMR ($CDCl_3$): δ ppm 0.91 (t, J = 7.22 Hz, 3H), 1.2−1.4 (m, 6H), 1.6−1.75 (m, 2H), 2.79 (t, J = 7.5 Hz, 2H), 5.15 (d, J = 10.8 Hz, 1H), 5.53 (d, J = 17.5 Hz, 1H), 6.67 (d, J = 2.7 Hz, 1H),6.75 (dd, J = 10.8/17.5 Hz, 1H), 6.86 (d, J = 3.5 Hz, 1H), 6.96−7.12 (m, 6H). ^{13}C NMR ($CDCl_3$): δ ppm 14.1, 22.6, 28.7, 29.7, 30.2, 31.5, 113.43, 123.5, 123.65, 123.70, 124.1, 124.3, 124.4, 124.9, 126.9, 129.7, 134.4, 135.1, 135.8, 136.1, 137.1, 142.1, 145.8, 153.6. Anal. Calcd for $C_{24}H_{24}S_4$: C, 65.41; H, 5.49. Found: C, 65.57; H, 5.47.

Poly(2-vinyl-5-methylthiophene), **PT1Me**. In a dry flask 0.813 g (6.6 mmol) of **12** and 0.014 g (0.0419 mmol) of benzoyl peroxide (BPO) were introduced. After flushing with dry N_2 for 1 h, five cycles of vacuum−N_2 were done. Then the mixture was heated in an oil bath to 90 °C and stirred under N_2 for 16 h. The crude oil obtained was dissolved in a minimum amount of CH_2Cl_2, and the solution was poured into 100 mL of methanol under stirring. The white-yellow precipitate was filtrated and suspended in fresh methanol for 1 h, then filtered, and washed with hexane. The product was dried in the oven overnight (50 °C), and 200 mg of a white-yellow solid (mp 195 °C) was obtained (25% yield). Gel permeation chromatography, ^{1}H NMR, and ^{13}C NMR characteristics are given in Table 1 and Figure 1. UV, PL, and PLE spectra are shown in Figures 2 and 3. The GPC plot is reported as Supporting Information.

Poly(5-vinyl-5′-methyl-2,2′-bithiophene), **PT2Me**. This polymer was prepared in the same way as **PT1Me**. After work up as described above, 114 mg of a yellow-orange solid were obtained (37% yield), mp 115 °C. GPC, ^{1}H and ^{13}C NMR characteristics are given in Table 1 and Figure 1. λ_{max} ($CHCl_3$) = 325 nm. The GPC plot is given as Supporting Information.

Poly(5-vinyl-5″-methyl-2,2′;5′,2″-terthiophene), **PT3Me**. A solution of 0.1 g (0.35 mmol) of **10** in dry toluene (2 mL) was degassed by several cycles of vacuum−N_2. Then 1 mol % of azobis(isobutyronitrile) (AIBN) was added. The solution was refluxed for 6 h, and then the viscous red mixture obtained was dissolved in a minimum amount of CH_2Cl_2 and poured into 30 mL of methanol under stirring to give a red-brown precipitate that was filtrated and suspended in fresh methanol overnight, then filtered, and washed with hexane. The product was dried in the oven overnight (50 °C), and 20 mg of red-brown polymer (mp 116 °C) was obtained (20% yield). Gel permeation chromathography, ^{1}H NMR, and ^{13}C NMR characteristics are given in Table 1 and Figure 1, while the UV−vis spectrum is shown in Figure 2. The GPC plot is reported as Supporting Information.

Poly(5-vinyl-5″-hexyl-2,2′:5′,2‴-terthiophene), **PT3Hex**. Compound **18** (0.11 g) was kept in air for 5 days, then dissolved in CH_2Cl_2, and poured into methanol (30 mL) under stirring to give a yellow precipitate. After washing with hexane 25 mg of polymer PT3HexA was collected (23% yield; mp >270 °C). Gel permeation chromatography, ^{1}H NMR, and ^{13}C NMR characteristics are given in Table 1. The GPC plot is given as Supporting Information, while the UV spectrum is shown in Figure 2.

Poly(5-vinyl-5‴-hexyl-2,2′:5′,2″:5″,2‴-quaterthiophene), **PT4-HexA.** This compound was obtained by spontaneous polymerization of monomer **22** and worked up in the same conditions used for **PT3Hex**. Gel permeation chromatography, ^{1}H NMR, and ^{13}C NMR characteristics are given in Table 1. The GPC plot is given as Supporting Information, while the UV spectrum is shown in Figure 2. The PL spectra in solution and in thin film are given in Figure 5.

Poly(5-vinyl-5‴-hexyl-2,2′:5′,2″:5″,2‴-quaterthiophene), **PT4-HexB**. This polymer was prepared following the procedure described above for **PT3Me**, starting from 0.18 g (0.41 mmol) of **22** and using 1 mol % of AIBN as radical initiator and dry toluene as the solvent (3 mL). The mixture was heated at 70 °C under nitrogen for 6 h, then 1 mol % AIBN was added again, and the mixture was stirred overnight. After 24 h two further additions of AIBN were made. Afterward, the solution was poured into 50 mL of methanol under stirring. After several washings of the solid precipitated, first with warm CH_2Cl_2 and then with distilled pentane, 0.072 g of polymer (as a dark brown powder) was isolated (40% yield; mp >260 °C). The proton NMR spectrum is described in Table 1. λ_{max} (CS_2) = 425 nm.

Gel permeation chromatography characterizations were carried out with a Shodex RI-71 (refractive index detection) system, with a single piston pump MSI Concept PU III, column PL Gel Mixed-E 0.3 mm porosity (polystyrene/divinylbenzene), eluted with toluene. Calibration plots were obtained from polystyrene standard solutions.

Photoluminescence and photoluminescence excitation measurements were performed with a JOBIN YVON Spex Fluorolog fluorimeter. Time-resolved PL measurements were made by using the second harmonic (390 nm) of a Ti−sapphire mode locked laser delivering 2 ps pulses at 82 MHz repetition rate. The luminescence was dispersed by a 0.24 m single monochromator coupled with a streak camera equipped

with a two-dimensional CCD. The overall time resolution was about 20 ps.

Optical microscopy observations were carried out with a Leica DMLS optical microscope.

Atomic Force Microscopy. All the AFM images were recorded with a stand-alone AFM (SMENA NT-MDT Moscow) operating in air, in noncontact mode (25° with relative humidity 55%). Si cantilever (NT-MDT NSG10, with typical curvature radius of a tip 10 nm and typical resonant frequency 255 kHz) were used. All images are unfiltered. The topographic images were corrected line-by-line for background trend effects by removal of the second-order polynomial fitting.

Computational Details. Molecular mechanics calculations were carried out using the MM3 (96) program.[26] Frontier orbitals and UV transitions were calculated by ZINDO/S-C.I. (8 × 8) single point calculations on optimized MM3 geometries using the HyperChem integrated package.[37]

Acknowledgment. This work was partially supported by the projects CNR-Agenzia 2000 and FIRB RBNE01YSR8. M. Benzi aknowledges support from Fondazione del Monte di Bologna e Ravenna. M. Cavallini acknowledges support from Project EU-G5RD-00349 MONA LISA.

Supporting Information Available: Synthesis of compounds **3**, **5**, **7**, **16**, and **19**, GPC plots of polymers, and a movie of crystals extinction. This material is available free of charge via the Internet at http://pubs.acs.org.

References and Notes

(1) *Science* **2002**, *295*, 2313−2556. Special issue on *Supramolecular Chemistry and Self-Assembly*. In particular: Lehn, J. M. *Science* **2002**, *295*, 2400−2402.
(2) Heeger, A. J. *Rev. Mod. Phys.* **2001**, *73*, 681−700.
(3) Köhler, A.; Wilson, J. S.; Friend, R. H. *Adv. Mater.* **2002**, *14*, 701−707.
(4) Dimitrakopoulos, C. D.; Malenfant, P. R. L. *Adv. Mater.* **2002**, *14*, 99−117.
(5) (a) Dodalabapur, A.; Torsi, L.; Katz, H. E. *Science* **1995**, *268*, 270−273. (b) Horowitz, G.; Garnier, F.; Yassar, A.; Hajlaoui, R.; Kouki, F. *Adv. Mater.* **1996**, *8*, 52−55. (c) Halik, M.; Klauk, H.; Zschieschang, U.; Schmid, G.; Ponomarenko, S.; Kyrchmeier, S.; Weber, W. *Adv. Mater.* **2003**, *15*, 917−922.
(6) (a) Garnier, F.; Hajlaoui, R.; El Kassmi, A.; Horowitz, G.; Laigre, L.; Porzio, W.; Armanini, M.; Provasoli, F. *Chem. Mater.* **1998**, *10*, 3334−3339. (b) Katz, H. E.; Lovinger, A. J.; Laquindanum, J. G. *Chem. Mater.* **1998**, *10*, 457−459. (c) H. E. Katz, Bao, Z. N.; Gilat, S. L. *Acc. Chem. Res.* **2001**, *34*, 359.
(7) Melucci, M.; Gazzano, M.; Barbarella, G.; Cavallini, M.; Biscarini, F.; Maccagnani, P.; Ostoja, P. *J. Am. Chem. Soc.* **2003**, *125*, 10266−10274.
(8) (a) Doi, H.; Kinoshita, M.; Okumoto, K.; Shirota, Y. *Chem. Mater.* **2003**, *15*, 1080−1089. (b) Mazzeo, M.; Vitale, V.; Della Sala, F.; Pisignano, D.; Anni, M.; Barbarella, G.; Favaretto, L.; Zanelli, A.; Cingolani, R.; Gigli, G. *Adv. Mater.* **2003**, *15*, 2060−2063. (c) Su, Y. Z.; Lin, J. T.; Tao, Y. T.; Ko, C. W.; Lin, S. C.; Sun, S. S. *Chem. Mater.* **2002**, *14*, 1884−1890.
(9) Pisignano, D.; Anni, M.; Gigli, G.; Cingolani, R.; Zavelani-Rossi, M.; Lanzani, G.; Barbarella, G.; Favaretto, L. *Appl. Phys. Lett.* **2003**, *81*, 3534−3536.
(10) (a) Antolini, L.; Horowitz, G.; Kouki, F.; Garnier, F. *Adv. Mater.* **1998.** *10*, 382−385. (b) Siegrist, T.; Kloc, C.; Laudise, R. A.; Katz, H. E.; Haddon, R. C. *Adv. Mater.* **1998**, *10*, 379−382. (c) Horowitz, G.; Bachet, B.; Yassar, A.; Lang, P.; Demanze, F.; Fave, J. L.; Garnier, F. *Chem. Mater.* **1995**, *7*, 1337−1341. (d) Siegrist, T.; Fleming, R. M.; Haddon, R. C.; Laudise, R. A.; Lovinger, A. J.; Katz, H. E.; Bridenbaugh, P.; Davis, D. D. *J. Mater. Res.* **1995**, *10*, 2170−2173. (e) Antolini, L.; Tedesco, E.; Barbarella, G.; Favaretto, L.; Sotgiu, G.; Zambianchi, M.; Casarini, D.; Gigli, G.; Cingolani, R. *J. Am. Chem. Soc.* **2000**, *122*, 9006−9013.
(11) Sessler, J. L.; Berthon-Gelloz, G.; Gale, P. A.; Camiolo, S.; Anslyn, E. V.; Anzenbacher, P., Jr.; Furuta, H.; Kirkovits, G. J.; Lynch, V. M.; Maeda, H.; Morosini, P.; Scherer, M.; Shriver, J.; Zimmerman, R. S. *Polyhedron* **2003**, *22*, 2063−2983.
(12) Marseglia, E. A.; Grepioni, F.; Tedesco, E.; Braga, D. *Mol. Cryst. Liq. Cryst.* **2000**, *348*, 137−151.
(13) Crystal, R. G. *Macromolecules* **1971**, *4*, 379−384.
(14) Yin, X. Y.; Ye, C.; Ma, X.; Chen, E. Q.; Qi, X. Y.; Duan, X. F.; Wan, X. H.; S. Cheng, Z. D.; Zhou, Q. F. *J. Am. Chem. Soc.* **2003**, *125*, 6854−6855.
(15) Nakano, T.; Yade, T. *J. Am. Chem. Soc.* **2003**, *125*, 15474−15484.
(16) Rathore, R.; Abdelwahed, S. H.; Guzei, I. A. *J. Am. Chem. Soc.* **2003**, *125*, 8712−8713.
(17) Trumbo, D. L. *Polym. Bull. (Berlin)* **1994**, *33*, 75−82.
(18) (a) Randazzo, M. E.; Toppare, L.; Fernandez, J. E. *Macromolecules* **1994**, *27*, 5102−5106. (b) O'Malley, R. M.; Randazzo, M. E.; Weinzierl, J. E.; Fernandez, L.; Nuwaysir, L. M.; Castoro, J. A.; Wilkins, C. L. *Macromolecules* **1994**, *27*, 5107−5113.
(19) (a) Nawa, K.; Imae, I.; Shirota, Y. *Macromolecules* **1995**, *28*, 723−729. (b) Imae, I.; Nawa, K.; Ohsedo, Y.; Noma, N.; Shirota, Y. *Macromolecules* **1997**, *30*, 380−386. (c) Imae, I.; Shirota, Y. *Synth. Met.* **1997**, *85*, 1385−1386. (d) Ohsedo, Y.; Imae, I.; Shirota, Y. *J. Polym. Sci., Part B: Polym. Phys.* **2003**, *41*, 2471−2484.
(20) Kagan, J.; Liu, H. *Synth. Met.* **1996**, *82*, 75−81.
(21) (a) Meeker, D. L.; Mudigonda, D. S. K.; Osborn, J. M.; Loveday, D. C.; Ferraris, J. P. *Macromolecules* **1998**, *31*, 2943−2946.
(22) Pagels, M.; Heinze, J.; Geschke, B.; Rang, V. *Electrochim. Acta* **2001**, *46*, 3943−3954.
(23) Hassan, J.; Sévignon, M.; Gozzi, C.; Schulz, E.; Lemaire, M. *Chem. Rev.* **2002**, *102*, 1359−1470.
(24) Melucci, M.; Barbarella, G.; Sotgiu, G. *J. Org. Chem.* **2002**, *67*, 8877−8884.
(25) (a) Chosrovian, H.; Rentsch, S.; Grebner, D.; Dahm, U.; Birckner, E. *Synth. Met.* **1993**, *60*, 23. (b) Kanemitsu, Y.; Suzuki, K.; Masumoto, Y.; Tomiuchi, Y.; Shiraishi, Y.; Kuroda, M. *Phys. Rev. B* **1994**, *50*, 2301. (c) A Grebner, D.; Helbig, M.; Rentsch, S. *J. Phys. Chem.* **1995**, *99*, 16991−16998. (d) Yassar, A.; Horowitz, G.; Valat, P.; Witgens, V.; Hmyene, M.; Deloffre, F.; Srivastava, P.; Lang, P.; Garnier, F. *J. Phys. Chem.* **1995**, *99*, 9155−9159. (e) Oelkrug, D.; Egelhaaf, H. J.; Gierschner, J.; Tompert, A. *Synth. Met.* **1996**, *76*, 249−253. (f) Yang, A.; Kuroda, M.; Shiraishi, I.; Kobayashi, T. *J. Chem. Phys.* **1998**, *109*, 8442−8450. (g) DiCésare, N.; Belletête, M.; Garcia, E. R.; Leclerc, M.; Durocher, G. *J. Phys. Chem. A* **1999**, *103*, 3864−3875.
(26) Allinger, N. L. *QCPE*; Indiana University; Bloomington, IN 47405.
(27) Tavazzi, S.; Borghesi, A.; Gurioli, M.; Meinardi, F.; Riva, D.; Sassella, A.; Tubino, R.; Garnier, F. *Synth. Met.* **2003**, *138*, 55−58.
(28) (a) Benedek, G. B.; Lastovka, J. B.; Fritsch, K.; Greytak, T. *J. Opt. Soc. Am.* **1964**, *54*, 1284. (b) Commission International de l' Eclairage (International Commission on Illumination), http://www.cie.co.at/cie/home.html. (c) The CIE Colour Space, http://hyperphysics.phy-astr.gsu.edu/hbase/vision/cie.html.
(29) (a) Bai, S. J.; Wu, C. C.; Dang, T. D.; Arnold, F. E.; Sakaran, B. *Appl. Phys. Lett.* **2004**, *84*, 1656−1658. (b) Tsai, M. L.; Liu, C. Y.; Hsu, M. A.; Chow, T. J. *Appl. Phys. Lett.* **2003**, *82*, 550−552.
(30) Hong, X. M.; Katz, H. E.; Lovinger, A. J.; Wang, B. B.; Raghachavari, K. *Chem. Mater.* **2001**, *13*, 4686−4691.
(31) Natta, G.; Pino, P.; Corradini, P.; Danusso, F.; Mantica, E.; Mazzanti, G.; Moraglio, G. *J. Am. Chem. Soc.* **1955**, *77*, 1708−1710.
(32) (a) Garnier, F.; Yassar, A.; Hajlaoui, R.; Horowitz, G.; Deloffre, F.; Servet, B.; Ries, S.; Alnot, P. *J. Am. Chem. Soc.* **1993**, *115*, 8716. (b) Amundson, K. R.; Katz, H. E.; Lovinger, A. J. *Thin Solid Films* **2003**, *426*, 140−149.
(33) D'Auria, M.; De Mico, A.; D'Onofrio, F.; Piancatelli, G. *J. Org. Chem.* **1987**, *52*, 5243−5247.
(34) Zotti, G.; Schiavon, G.; Berlin, A.; Pagani, G. *Chem. Mater.* **1993**, *5*, 430−436.
(35) Benson, D.; Karsch-Mizrachi, I.; Lipman, D. J.; Ostell, J.; Rapp, B. A.; Wheeler, D. L.; Genbank, D. L. *Nucleic Acids Res.* **2000**, *28*, 15−18.
(36) Barbarella, G.; Favaretto, L.; Sotgiu, G.; Zambianchi, M.; Antolini, L.; Pudova, O.; Bongini, A. *J. Org. Chem.* **1998**, *63*, 5497−5506.
(37) *HyperChem rel 7.0* from Hypercube, Inc., Waterloo, Ontario, Canada.

MA049102Q